



OPEN ACCESS

EDITED BY

Guoqi Han,
Fisheries and Oceans Canada (DFO),
Ottawa, Canada

REVIEWED BY

Junde Li,
Hohai University, China
Agus Setiawan,
National Research and Innovation Agency,
Indonesia
Guangjun Xu,
Guangdong Ocean University, China

*CORRESPONDENCE

Yaru Guo

✉ yaruguo@qdio.ac.cn

Fan Wang

✉ fwang@qdio.ac.cn

RECEIVED 22 October 2023

ACCEPTED 28 November 2023

PUBLISHED 11 December 2023

CITATION

Guo Y, Li Y, Yang D, Li Y, Wang F and
Gao G (2023) Water sources of the
Lombok, Ombai and Timor outflows of the
Indonesian throughflow.
Front. Mar. Sci. 10:1326048.
doi: 10.3389/fmars.2023.1326048

COPYRIGHT

© 2023 Guo, Li, Yang, Li, Wang and Gao.
This is an open-access article distributed
under the terms of the [Creative Commons
Attribution License \(CC BY\)](https://creativecommons.org/licenses/by/4.0/). The use,
distribution or reproduction in other
forums is permitted, provided the original
author(s) and the copyright owner(s) are
credited and that the original publication in
this journal is cited, in accordance with
accepted academic practice. No use,
distribution or reproduction is permitted
which does not comply with these terms.

Water sources of the Lombok, Ombai and Timor outflows of the Indonesian throughflow

Yaru Guo^{1*}, Yuanlong Li^{1,2}, Dezhou Yang^{1,2}, Yuxuan Li¹,
Fan Wang^{1,2*} and Guandong Gao^{1,2}

¹CAS Key Laboratory of Ocean Circulation and Waves, Institute of Oceanology, Chinese Academy of Sciences, Qingdao, China, ²Laoshan Laboratory, Qingdao, China

The Lombok Strait (LS), Ombai Strait (OS), and Timor Passage (TP) are three major outlets of the Indonesian Throughflow to the Indian Ocean. Here, sources and pathways of the LS, OS, and TP outflows are explored by a Lagrangian particle tracking analysis based on a ~3 km regional ocean model simulation. The Makassar Strait transport contributes to ~80%, ~75%, and ~45% of the LS, OS, and TP outflows, respectively. However, ~41% and ~19% of the TP and OS outflows stem from the Lifamatola Passage, which largely feeds the upper and intermediate layers of the outflows. The role of Karimata Strait is quite limited and restricted to the upper layer. It takes 1-2 years and 2-6 years for the Makassar Strait water to reach the OS and TP, respectively, whereas the Lifamatola Passage water passes through the OS (2-6 years) and TP (3-9 years) on a prolonged transit time. In the Banda Sea, the western boundary current is the main pathway toward the OS, while the waters to the TP tend to take a basin interior route.

KEYWORDS

the Indonesian throughflow, Indonesian seas, lagrangian particle tracking, Makassar strait, Lifamatola passage

1 Introduction

The low-latitudes Pacific Ocean water can penetrate to the Indian Ocean through the Indonesian Seas (Wyrcki, 1961; Gordon and Fine, 1996; Hautala et al., 1996). This connectivity fundamentally affects the heat and freshwater budgets and air-sea heat fluxes of the Pacific and Indian Oceans and behaviors of the El Niño/Southern Oscillation (ENSO) and Asian monsoons (Godfrey, 1996; Wajsovicz and Schneider, 2001; Lee et al., 2002; Vranes et al., 2002; Taufiqurrahman et al., 2020). In the Indonesian Seas, the Pacific-origin water follows complex pathways and exits through three major outlets, i.e., the Lombok Strait (LS), Ombai Strait (OS), and Timor Passage (TP), forming a relatively stable transport of >10 Sv known as the Indonesian throughflow (ITF; Wyrcki, 1961; Fioux et al., 1994).

Pathways of the ITF within the Indonesian Seas are divided into three major routes: the shallow western route through the Karimata Strait (Qu et al., 2005; Qu et al., 2006; Tozuka

et al., 2009; Fang et al., 2010; Gordon et al., 2012; Susanto et al., 2012; Susanto et al., 2013), the central route through the Makassar Strait (Gordon and Fine, 1996; Wajsowicz, 1996; Susanto and Gordon, 2005; Pujiana et al., 2009; Gordon et al., 2010) with a sill depth of ~680 m (Gordon et al., 1999; Gordon et al., 2003; Qu et al., 2009), and the deeper eastern route through the Lifamatola Passage and Halmahera Sea (Van Aken et al., 2009; Wang et al., 2018; Wang et al., 2019; Yuan et al., 2022). Makassar Strait transport accounts for 77% of the thermocline-intensified ITF (Gordon and Fine, 1996; Gordon, 2005; Gordon et al., 2008; Gordon et al., 2010), while the Lifamatola Passage east of Sulawesi serves as a main path for the intermediate and deep Pacific Ocean waters to the Indonesian Seas, giving rise to a deep-layer branch of the throughflow (Miyama et al., 1995; Van Aken et al., 2009; Wang et al., 2018; Wattimena et al., 2018). In comparison, the Karimata Strait is supposed to have a smaller contribution to the total ITF transport (Wang et al., 2006; Susanto et al., 2013), although with a notable impact on the ITF's seasonal and interannual variability (e.g., Qu et al., 2006; Gordon et al., 2012; Lee et al., 2019). Despite existing knowledge, quantitative understanding of the water partition among these pathways remains lacking.

The Makassar Strait, as the leading source, feeds all the major flow pathways out of the Indonesian Seas. There is a short conduit

from the Makassar Strait to the LS with identifiable Pacific-water signatures and a lengthened path toward the TP with water properties modified by mixing (Figure 1; Atmadipoera et al., 2009). The Lifamatola Passage ventilates the intermediate water of the Banda Sea, which exits through the OS and TP (Gordon and Fine, 1996; Molcard et al., 2001; Gordon, 2005). The lack of LS destination of the Lifamatola Passage water is likely caused by the blocking of the shallow Dewakang Sill in the southern Makassar Strait (Gordon et al., 2003). The Karimata Strait throughflow provides the low-salinity surface water and attenuates the surface ITF during the boreal winter via a “freshwater plug” at the southern tip of the Makassar Strait (Lebedev and Yaremchuk, 2000; Qu et al., 2005; Tozuka et al., 2007; Fang et al., 2009; Qu et al., 2009; Gordon et al., 2012).

Pathways of the ITF water within the Indonesian Seas are important in many senses. For example, by transporting nutrients and dissolved oxygen, the pathways are essential in supporting marine ecosystems and the biodiversity pattern of the Coral Triangle (Sprintall et al., 2014), affecting the behavior, migration pattern of the fish species (Sprintall et al., 2019) and the food supply and livelihood of the surrounding countries. In addition, the outflows at the LS, OS, and TP are different in vertical structures and water properties (Atmadipoera et al., 2009; Sprintall et al.,

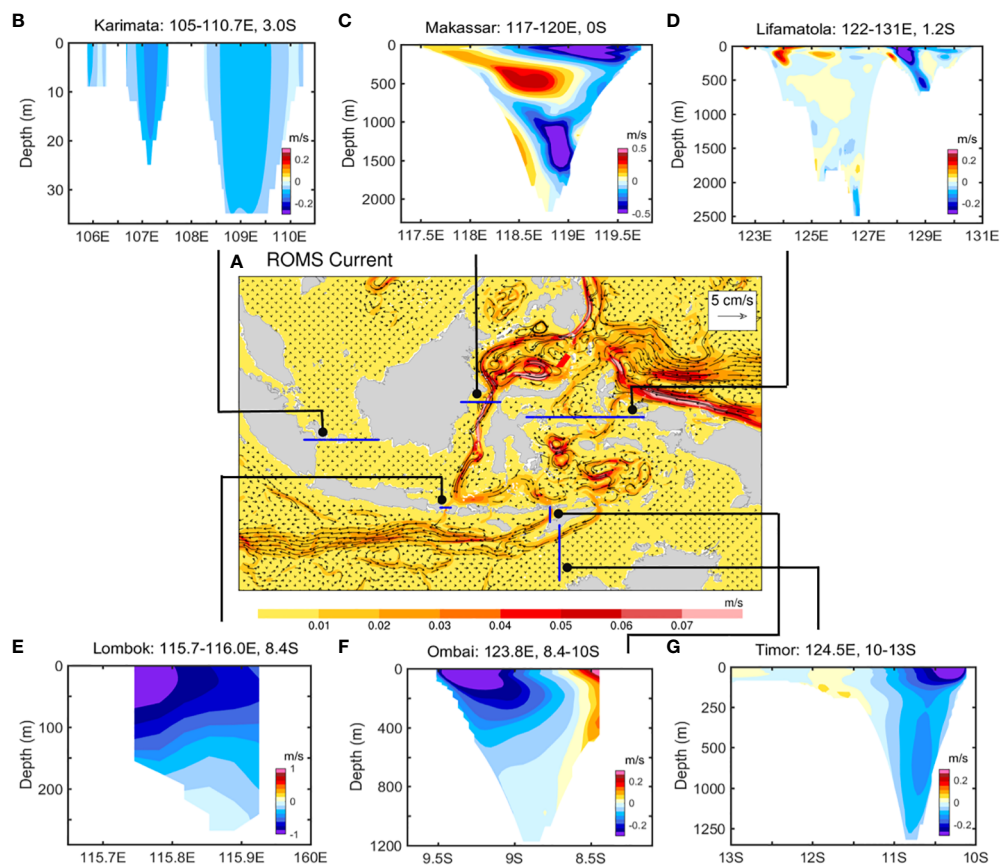


FIGURE 1 (A) Full-depth averaged ocean current vectors (cm/s) and magnitude (m/s), along with the annual climatological velocity (m/s) sections at the (B) Karimata Strait, (C) Makassar Strait, (D) Lifamatola Passage, (E) Lombok Strait (LS), (F) Ombai Strait (OS), and (G) Timor Passage (TP), derived from the ~3 km ROMS simulation.

2019) and exert complex impacts on the thermocline layer structure of the ITF, the circulation pattern, and the biogeochemical cycles of the Southeast Indian Ocean. With these regards, water sources and pathways of the LS, OS, and TP outflows are worthy of in-depth investigation.

This study attempts to understand sources and pathways of the ITF outflow by conducting Lagrangian particle tracking analysis using three-dimensional ocean velocity fields derived from a ~3 km regional ocean model simulation. The water through the Karimata Strait, Makassar Strait, and Lifamatola Passage (extended eastward to include the inflows from the Halmahera Sea) are considered as candidate water sources for the LS, OS, and TP outflows (Figure 1).

2 Model and data

2.1 Model

Three-dimensional velocity fields are simulated by the Regional Ocean Modeling System (ROMS), which is a state-of-the-art hydrostatic, primitive equation ocean model that implements a free-surface, a vertical terrain-following coordinate system, and horizontal curvilinear coordinate (Haidvogel et al., 2000). In this work, the model covers a domain between 69°-165°E and 21°S-51°N with a ~3 km horizontal resolution and 50 terrain-following layers. The model topography is extracted from a combination of Earth topography one-minute and five-minute resolutions, along with manually smoothing and adding part of islands (Shchepetkin and McWilliams, 2005). The model is driven by the climatological monthly open boundary conditions from the Hybrid Coordinate Ocean Model datasets (Bleck et al., 2002) and the climatological initial conditions from the World Ocean Atlas 2013 dataset (Locarnini et al., 2013), involving the current, temperature and salinity information. The monthly climatology mean heat flux, wind stress, and freshwater flux are derived from the Comprehensive ocean-Atmosphere Data Set (Diaz et al., 2002). The Smagorinsky and K-profile parameterization schemes are adopted to obtain the horizontal and vertical eddy viscosities, respectively. The model is forced by 10 tidal constituents originating from the TPXO8 (Egbert and Erofeeva, 2002). A spin-up integration of 15 years was conducted under monthly climatology forcing fields and open boundary conditions, in which the climatological three-dimensional velocity fields in the last year, stored as a 5-day average, are to be used to track the ITF water. Detailed descriptions of the model configuration have been provided by Gao et al. (2022).

The ROMS simulation analyzed here is updated from that of Gao et al. (2022) by slightly modifying the land-sea geometry to improve the representation of ITF. Intense tidal mixing in the Indonesian Seas is shown to modify the temperature-salinity properties of the Pacific water (Iskandar et al., 2023). As such, internal tides are identified as the leading driver for the water mass transformation (Koch-Larrouy et al., 2008). The simulated amplitude and phases of the major tidal constituents M2 and K1 by ROMS are well matched with the TOPEX/POSEIDON crossover data from Robertson and Ffield (2008), with a high correlation

(Figure S1). The passage transports have been verified in our previous study (Gao et al., 2022), and further validations relevant to the critical straits are here. The along-strait velocity observations of the LS and TP are well reproduced by ROMS, although the OS overflow from July to August and the southward Makassar flow from 200 to 600 m are slightly underestimated (Figures S2, S3). The Makassar Strait features a three-layer vertical structure, yielding a volume transport of 15.41 Sv close to observations (Figure 1; Sprintall et al., 2009). Along this velocity section, the southward-flowing water will either pass through three outlet straits or reside in the Indonesian Seas. It's hard for the climatology northward-flowing water to be tracked as source water and affect the ITF outflow. The western intensification of LS, the southern intensification of OS with the upper opposite south-north currents, and the surface-intensified TP are well represented, resulting in similar estimates of 2.69, 4.92, and 7.96 Sv as observations (Hautala et al., 2001; Liang et al., 2019). These comparisons, combined with previous validations, suggest that ROMS simulation is suitable for our analysis.

2.2 CMS Lagrangian analysis

The Connectivity Modeling System (CMS) version 2.0 (Paris et al., 2013) is applied to Eulerian three-dimensional velocity fields to conduct a Lagrangian description through the offline backward tracking of the particles in time. A fourth-order Runge-Kutta scheme is used for time stepping, in which particle trajectories are interpreted as stream tubes to warrant the tagged transport as a constant during transit owing to the nearly incompressible nature of seawater (Blanke and Raynaud, 1997). An individual particle can be initially tagged with a particular volume transport that keeps constant both forward and backward in time. Therefore, the Lagrangian connectivity is quantified by summing the infinitesimal transports of the particles passing through the predefined sections, and the CMS tracking algorithm is an efficient tool for estimating the water transport. The CMS can augment specific features by adding different modules, extensively enhancing its application (Weijer et al., 2012; Qin et al., 2014; van Sebille et al., 2014; Cheng et al., 2016). The turbulence and vertical mixing (mostly tides) in the Indonesian Seas are of importance to ocean circulation and volume transport and transit time of the ITF (Ffield and Gordon, 1992; Qu et al., 2009). Hence, it is essential to turn on the CMS turbulent module that can introduce random perturbations into the particle trajectories to modulate the water movement. More details regarding CMS turbulent mixing can refer to Brickman and Taylor (2007) and Guo et al. (2023).

2.3 Experiments

For ROMS simulation, the particles are seeded at all model grid cells over the whole water column along the initial sections of the LS (115.7-116.0°E, 8.4°S), OS (123.8°E, 8.4-10.0°S), and TP (124.5°E, 10.0-13.0°S) at 5-day intervals for a quasi-steady period of 1 year (Figure 1). With the opening of the CMS turbulent module using a

typical diffusivity coefficient of $0.1 \text{ m}^2 \text{ s}^{-1}$ and a perturbation frequency of one time-step (Cheng et al., 2016; Guo et al., 2023), each grid point possesses 10 members to quantify the potential uncertainty by the inter-member spread. There are a total of 113860, 837920, and 2065170 particles released in the LS, OS, and TP, respectively. Each particle is assigned a partial transport representing the volume flux through the grid cell. All particles are tracked backward for 20 years by repeatedly looping three-dimensional velocity fields derived from the last year of the 15 years integration, following previous practices (van Sebille et al., 2012; R hls et al., 2013; Durgadoo et al., 2017). Particle positions are stored every 2 days.

3 Results

3.1 Water sources

The sources of LS, OS, and TP outflows are first examined (Figure 2). As soon as the water passes the Karimata, Makassar, and Lifamatola sections or enters the Indian Ocean across the repeated expendable bathythermograph IX1 line, the tracking is terminated. The mean transport of the Makassar Strait into the LS is 2.15 Sv based on the ensemble mean of 10 members, along with an uncertainty of ~ 0.01 Sv. Thereby, the Makassar Strait origin is able to account for the LS transport of up to $\sim 80.0\%$, illustrating its dominant role (Figure 2A). The Karimata Strait origin is of secondary importance, explaining $\sim 8.2\%$ of the outflow (0.22 ± 0.01 Sv), while the remaining outflow of the LS ($\sim 11.9\%$) is extracted from the interior of Indonesian Seas. Note that the source water of Lifamatola Passage fails to the LS, as previously

analyzed (Gordon et al., 2003). The leading entrance channelling the Pacific water through the OS is the Makassar Strait, transporting an outflow of 3.68 ± 0.02 Sv ($\sim 74.8\%$; Figure 2C). The Lifamatola Strait is identified as another critical source, providing the transport of 0.91 ± 0.01 Sv ($\sim 18.5\%$), whereas the Karimata Strait ($\sim 1.4\%$) and the Indonesian Seas origins ($\sim 5.1\%$) can be neglected. The Indian Ocean inflows, minimally reaching the OS (~ 0.01 Sv) and TP (~ 0.03 Sv), are not shown.

The Makassar Strait and Lifamatola Passage origins are of comparable importance to the TP outflow, yielding contributions of $\sim 44.6\%$ (3.55 ± 0.02 Sv) and $\sim 40.7\%$ (3.24 ± 0.02 Sv), respectively (Figure 2E). Given the sparse observations (Sprintall et al., 2019), the Lifamatola Passage yields a wide range of transport estimates from -0.8 to 5.2 Sv (e.g., Luick and Cresswell, 2001; Talley and Sprintall, 2005; Van Aken et al., 2009), leading to its role not being accurately evaluated before. This study produced for the first time a quantitative understanding of the contribution of Lifamatola Passage to the ITF based on the water tracking algorithm. The relative contribution of Karimata Strait origin to the TP outflow is quite limited (0.06 ± 0.01 Sv, $\sim 1.0\%$), while there is a portion of the outflow originating from the internal Indonesian Seas (1.08 ± 0.02 Sv, $\sim 13.6\%$). These results indicate the first-order importance of the Makassar Strait origin, but more importantly, the Lifamatola Strait is an essential source of the OS and TP outflows and deserves to be taken seriously. It appears that the turbulence-induced uncertainties are two orders of magnitude smaller than the average transports, illustrating the minor influence of the mixing on the ITF transport and agreeing well with a previous study (Iskandar et al., 2023), and therefore not considered below.

The transit time indicates the time for the source water of ITF to reach the export straits. The minimum travelling time generally

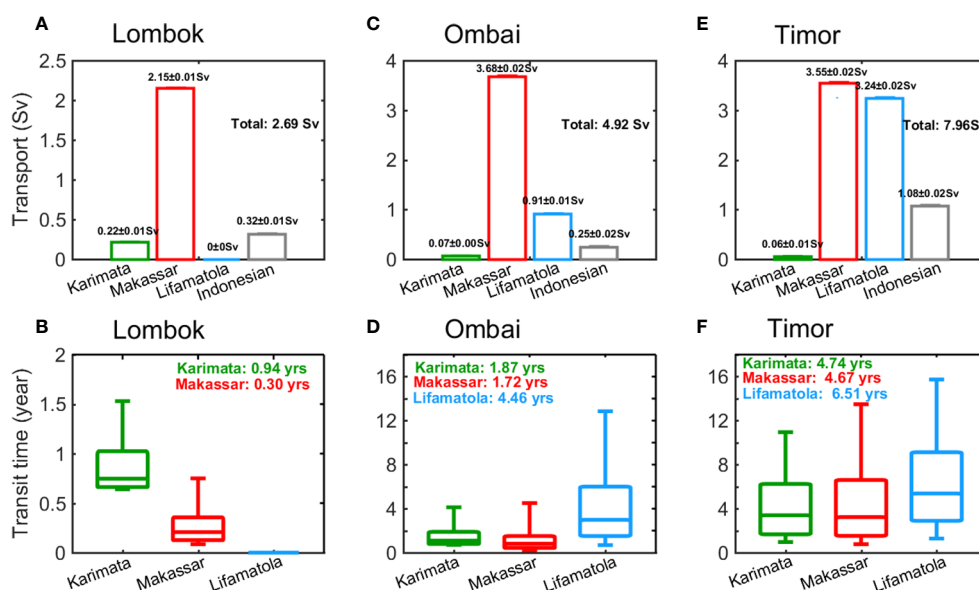


FIGURE 2

The transports (Sv) traced back to the Karimata Strait, Makassar Strait, Lifamatola Passage, and remained within the Indonesian Seas for the water particles released at the (A) LS, (C) OS, and (E) TP, derived from the ROMS simulation. (B, D, F) Same as (A, C, E), but for transit time (year). The boxes denote the 25th, 50th, and 75th percentiles, while the tails indicate the 10th and 90th percentiles. The transports at exit straits and the mean traveling time are embedded.

occurs over the LS, whereas the opposite situation emerges in the TP (Figure 2). Specifically, around half of the Karimata Strait water (between the 25th and 75th percentiles) transits to the LS, OS, and TP for 0.7-1 year, 1-2 years, and 2-6 years, respectively. The Makassar Strait inflow yields roughly the same results but takes a shortened traveling time to the LS (0.1-0.4 years) as the more direct connectivity between them (Koch-Larrouy et al., 2008). By contrast, a prolonged transit time for the Lifamatola Passage inflow is 2-6 years to the OS and 3-9 years to the TP. A close inspection over all time boxes shows extraordinarily long upper tails probably induced by the complex pathways associated with multiple dynamic factors, such as the monsoonal winds and the highly energetic mesoscale eddy field (Koch-Larrouy et al., 2008; Purba and Khan, 2019), and a detailed analysis is provided as follows.

3.2 Vertical structure

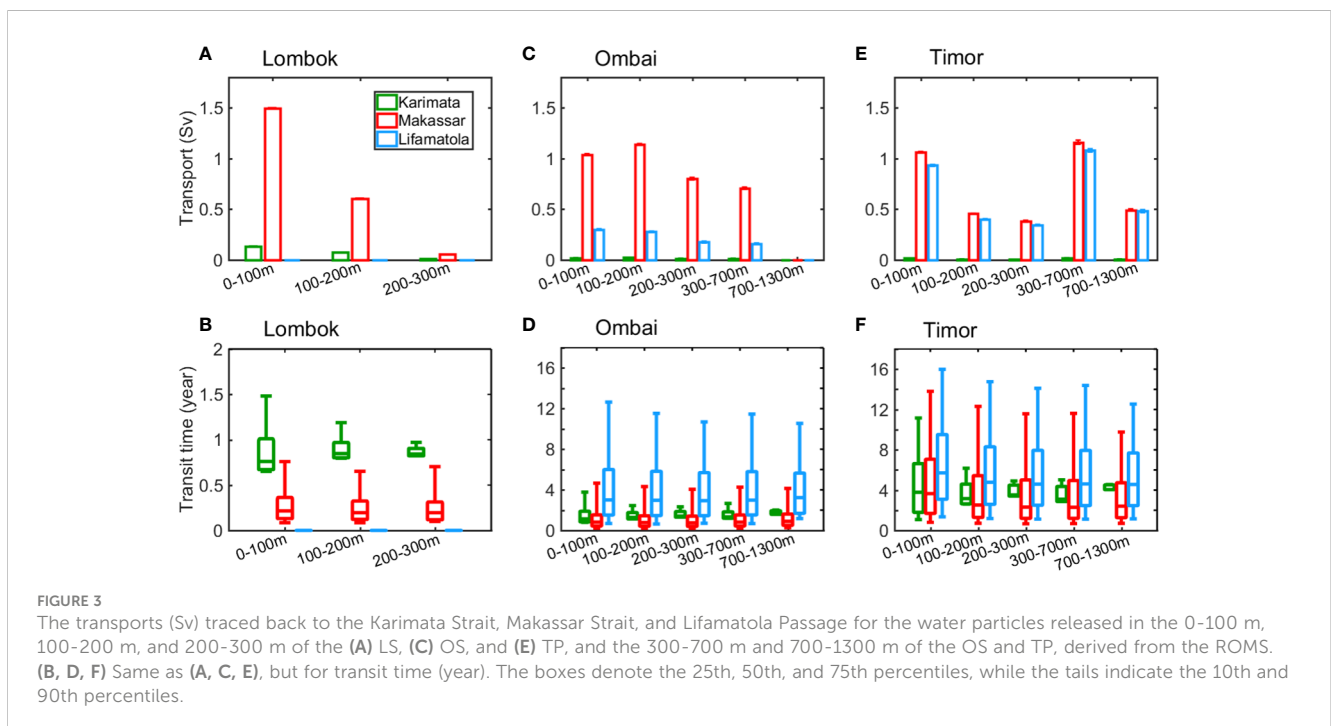
In this section, we attempt to examine the discrepancies among layers. The LS outflow features surface intensification, originating mainly from the Makassar Strait inflow and minimally from the Karimata Passage inflow at each depth (Figure 3A). Worth noting is that the layered inflows here refer to the vertical distributions at the LS, OS, and TP, a consequence after the transit within the Indonesian Seas. The OS transport maxima in the upper 200 m are a combined action of the thermocline-intensified Makassar Strait and the surface-intensified Lifamatola Passage inflows (Figure 3C). The surface enhancement of the Lifamatola Passage water is likely drawn from the Halmahera Strait that allows the shallow Pacific water to enter the Indonesian Sea and then composes the upper Banda Sea (Gordon et al., 2003; Potemra et al., 2003; Liang et al., 2019). Compared with Makassar Strait,

the Lifamatola Passage displays approximately equal contributions to the TP transport at each depth level, causing the maximum confined to the top 100 m but the intermediate maximum as the cumulative effect of multiple layers (Figure 3E). The intermediate enhancement of Lifamatola Passage inflow probably stems from the observed intermediate and deep currents through this passage (Van Aken et al., 2009; Yuan et al., 2022), intruding into the Banda Seas in which the water manifests as an elevated mixture by vigorous mixing with the ambient water (Van Aken et al., 1988; Field and Gordon, 1996). As such, the Lifamatola Passage offers a significant source for the ITF throughout the entire depth, especially the upper and intermediate layers of ITF outlets.

We further examine the transit time from the sources to the outlets of ITF. There exist extended time spans for the Karimata Strait inflow to pass through the upper layers of the three outlets (0.6-1.5 years, 1.0-4.0 years, and 1.6-11.8 years for the LS, OS, and TP, respectively), in contrast to the bottom levels (0.8-1.0 years, 1.8-2.0 years, and 4.0-4.1 years for the LS, OS, and TP, respectively), most notably at the tops of the time boxes (Figure 3). This difference is due predominantly to the upper water of Karimata Strait more easily switching into the southern Makassar Strait driven by the monsoon winds (Qu et al., 2009), as a comparison of the slowest trajectories between the upper and lower layers of 100 m at the LS (Figures 4A, C), and the modulation of upper-ocean high eddy activities that cover the whole Indonesian Seas except the Java Sea (Figures 4B, D), resembling previous distributions (Purba et al., 2020; Iskandar et al., 2023). The eddy kinetic energy (EKE) is calculated as follows:

$$EKE = \frac{1}{2}(u'^2 + v'^2)$$

where u' and v' are the zonal and meridional current anomalies by subtracting their respective seasonal variations from the zonal



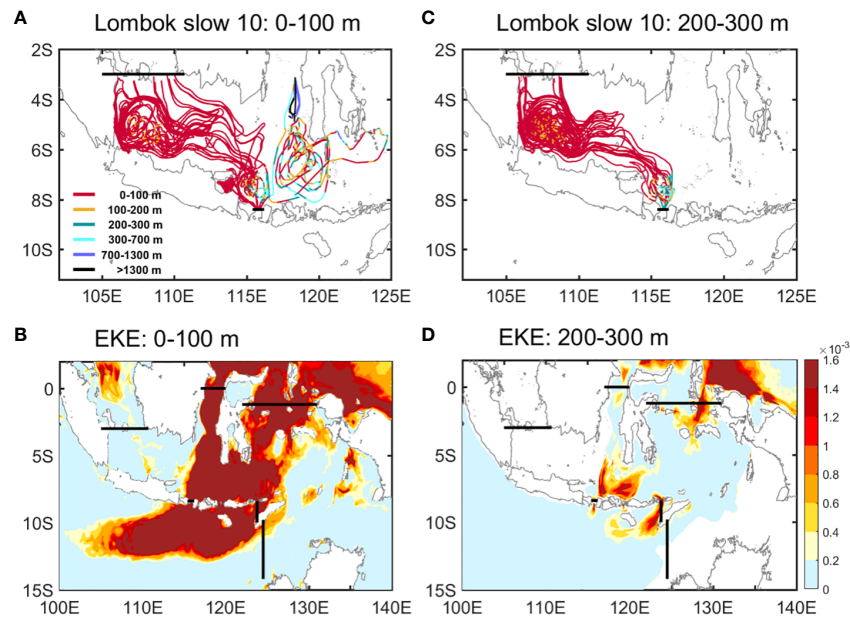


FIGURE 4 The slowest 10 trajectories of the Karimata Strait water to the (A) top 100 m and (C) 200–300 m of the LS. Different colors represent different depth levels. Mean maps of eddy kinetic energy (EKE, $m^2 s^{-2}$) in (B) the 0–100 m and (D) 200–300 m. The results are derived from the ROMS.

and meridional velocities (Richardson, 1983). Also, the TP outflow between layers takes an approximately equal transit time back to the Makassar and Lifamatola Straits (Figure 3F). This is primarily induced by the strengthened intermediate and bottom flows through the Lifamatola Passage (Van Aken et al., 2009; Yuan et al., 2022) and the different flowing trajectories for the upper and bottom layers of the TP, in which the former additionally contains the westward flow, related to the Australian monsoon,

towards the Indian Ocean during backward tracking (Figure S4; Masumoto and Yamagata, 1996).

3.3 Pathways

The fastest trajectories of the source water are usually concentrated along a uniform pathway, while the median

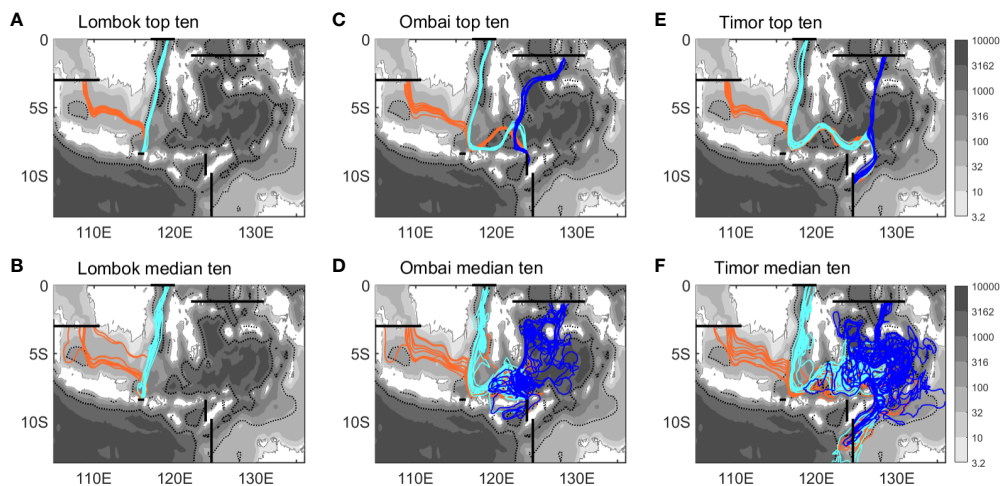


FIGURE 5 (A) The fastest and (B) median 10 trajectories from the Karimata (orange) and Makassar Straits (cyan) to the LS, derived from the ROMS. (C, D) are the same as (A, B) but for the trajectories from the Karimata Strait (orange), Makassar Strait (cyan), and Lifamatola Passage (blue) to the OS. (E, F) are the same as (C, D) but for trajectories to the TP. Gray filling represents water depths, with an emphasis on 100 (thin dashed line) and 1000 m (thick dashed line).

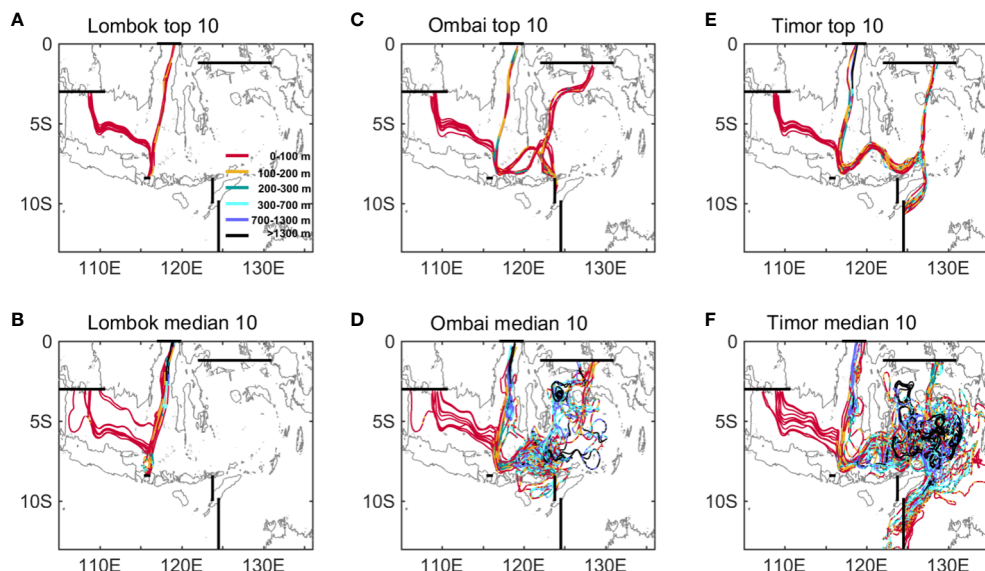


FIGURE 6

(A) The fastest and (B) medium 10 trajectories of the Karimata and Makassar Strait inflows to the LS, derived from ROMS. Different colors represent different depth levels. (C, D) are the same as (A, B), but for the Karimata Strait, Makassar Strait, and Lifamatola Passage water to the OS. (E, F) are the same as (C, D) but for the TP.

trajectories often additionally contain multiple loops and significant vertical motions (Figures 5, 6). For the former, the southward-flowing Karimata Strait water tends to parallel the isobath and bifurcates in the southern Makassar Strait. In addition to the LS branch, the eastward branch proceeds along the southern island chain of the Indonesian Seas and conducts a northward detour along 1000 m isobath to bypass the deep Flores Sea, subsequently impinging upon the western Sulawesi and returning to the south by local prevailing upwelling (Purba and Khan, 2019), finally exporting through the OS and TP (Figure 5). The flow is confined to the top 100 m during transit (Figure 6). However, the moderate trajectories become more irregular and induce stronger vertical motions.

The Makassar Strait source water generally originates from the eastern side of the strait but is centrally located at various depths for the LS (0–100 m), OS (0–300 m), and TP destinations (full depth) along the fastest trajectories (Figures 5, 6). The Makassar jet travels southward along the 100 m isobath, which partly enters the LS. The eastward upper branch undergoes a sizeable northward detour near the eastern Sulawesi before reaching the OS, accompanied by notably ascending and descending signals (Figures 5C, 6C). It appears that the turning position of the Makassar Strait water differs drastically from that of the Karimata Strait inflow, while their median trajectories yield the same detours (Figures 5D, 6D). To explore the reason, the month evolutions of the trajectories of the Karimata and Makassar Strait inflows into the OS are given in Figure 7. The inflows suffering the northward detour over the western Sulawesi reach the OS during August–September (Figure 7A), corresponding to the occurrence time of OS transport maximum based on previous analysis (Sprintall et al.,

2009). However, the trajectories with a detour further east pass through the OS during March–April (Figure 7B), which is likely related to the wind-driven eastward advection. Thus, the pathways of the ITF in the Indonesian Seas are highly correlated with the seasonality of the outflows and probably regulate the season-related biogeochemical signatures during transit.

The remaining eastward branch originating from the full-depth Makassar Strait follows the same northward steering as the Karimata Strait inflow to the TP for both the uniform fastest and complex medium trajectories (Figures 5, 6). In this situation, the inflows drawn from the Karimata and Makassar Straits reach the TP simultaneously, that is, during boreal summer (Figure 7). The close connection between the varying pathways and seasonal variability is further confirmed.

The Lifamatola Passage provides its origins of the OS outflow mainly in the 0–100 m and the TP outflow in the 0–700 m for the fastest trajectories (Figures 6C, E). The inflowing water travels to the OS through the western boundary of the Banda Sea, paralleling the 1000 m isobath and restricted within the 0–200 m levels. By contrast, the water transit to the TP is through the central Banda Sea with a shallow depth. However, the median trajectories feature deeper water sources and more intricate trajectories (Figures 6D, F). The inflow splits into two branches to enter the OS, one propagating southward with the support of the intermediate and bottom western boundary current of the Banda Sea (Van Aken et al., 2009; Yuan et al., 2022) and the other across the shallow interior of Banda Sea. During transit to the TP, the pathways interweave with each other, resulting in evidently rising and falling processes (Figures 5F, 6F). Thus, the source water in the Indonesian Seas tends to choose a

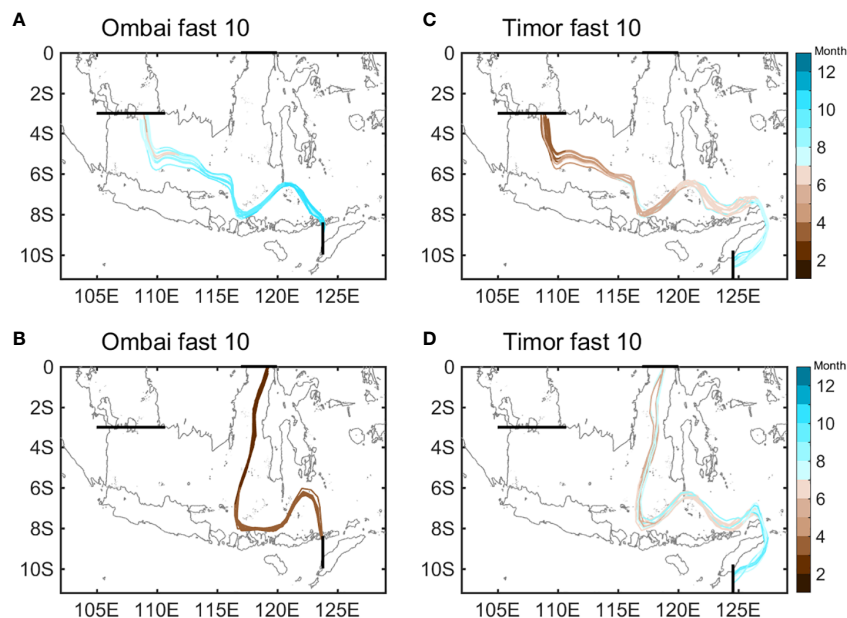


FIGURE 7
Month evolution with the transit along the fastest trajectories of the (A) Karimata Strait and (B) Makassar Strait waters to the OS, derived from the ROMS. (C, D) are the same as (A, B) but for the TP.

shallower depth or depend on a stronger current to quickly arrive at the three outlets of ITF and the Indian Ocean.

4 Summary and discussion

The ITF exits the Indonesian Seas to the Indian Ocean mainly via the LS, OS, and TP. The water sources and pathways of the three outflows are explored by conducting backward Lagrangian particle tracking experiments in the high-resolution (~ 3 km) ROMS velocity fields. The results confirm the dominance of Makassar Strait origin, explaining $\sim 80\%$, $\sim 75\%$, and $\sim 45\%$ of the LS, OS, and TP outflows, respectively, and concentrating on the thermocline and its upper layers. The Lifamatola Passage, as an essential source, devotes $\sim 41\%$ of the TP outflow by primarily offering the upper and intermediate outflows and $\sim 19\%$ of the OS transports by mainly providing the upper outflow. The Karimata Strait contribution is quite limited and confined to the upper layer. Owing to the monsoon reversals and upper-ocean substantial eddy activities, the Karimata Strait inflow reaches the LS, OS, and TP on an average of 0.7-1 year, 1-2 years, and 2-6 years, respectively. The same transit time is obtained for the Makassar Strait inflow but for a shortened time into the LS (0.1-0.4 years) as the shorter route. The Lifamatola Passage inflow takes a longer time to the OS (2-6 years) and the TP (3-9 years). The Karimata and Makassar Strait inflows generally undergo different northward detours near the Flores Sea before passing through OS and TP, with implications for the seasonality of ITF transport. The Lifamatola Passage water exits through the OS and TP by the strong western boundary currents and the shallow interior of the Banda Sea, respectively.

Lifamatola Passage throughflow may exert a considerable influence on the local climate based on previous studies (Van Aken et al., 2009), while its transport estimates remain limited. The most striking result of this work is to highlight the prominent importance of the Lifamatola Passage origin for the ITF transport and quantify its contributions to the outflows of the two main export channels. Although the mean sources of the ITF outflow have been identified in the present study, knowledge gaps remain in their seasonal to interannual variability. This unresolved issue deserves careful consideration because the ocean circulation and dynamics in the Indonesian Seas are thought to be the results of the nonlinear interplay between monsoonal winds, ENSO, Indian Ocean Dipole, and topography (Kartadikaria et al., 2012; Sprintall et al., 2014). For example, the anomalously easterly winds in the Java Sea region during the peak of 1997/98 El Niño and positive Indian Ocean Dipole induce coastal upwelling south of Sumatra-Java and subsequently the weaker northward flow of the Makassar Strait (Susanto and Gordon, 2005). In addition, the Kelvin waves in response to the Indian Ocean monsoon transitions propagate eastward to the Sumatra and the ITF three export straits, which induces the semiannual reversals of ITF outflow and a weakening of the Makassar Strait throughflow (Gordon et al., 2008; Sprintall et al., 2009).

Data availability statement

The original contributions presented in the study are included in the article/Supplementary Materials. Further inquiries can be directed to the corresponding authors.

Author contributions

YG: Data curation, Software, Writing – original draft, Writing – review & editing. YLL: Formal Analysis, Writing – review & editing. DY: Data curation, Writing – review & editing, Validation. YXL: Validation, Writing – review & editing. FW: Writing – review & editing. GG: Validation, Writing – review & editing.

Funding

The author(s) declare financial support was received for the research, authorship, and/or publication of this article. This work is supported by the Strategic Priority Research Program of CAS (XDB42000000), the National Key R&D Program of China (2019YFA0606702), the China Postdoctoral Science Foundation (2022M723182), the Shandong Province Postdoctoral Innovation Project (E3KY171), the Shandong Natural Science Foundation Youth Program (ZR2023QD114), and the Oceanographic Data Center, IOCAS.

References

- Atmadipoera, A., Molcard, R., Madec, R., Wijffels, S., Sprintall, J., Koch-Larrouy, A., et al. (2009). Characteristics and variability of the Indonesian throughflow water at the outflow straits. *Deep Sea Res. Part I* 56, 1942–1954. doi: 10.1016/j.dsr.2009.06.004
- Blanke, B., and Raynaud, S. (1997). Kinematics of the Pacific equatorial undercurrent: an Eulerian and Lagrangian approach from GCM results. *J. Phys. Oceanogr.* 27, 1038–1053. doi: 10.1175/1520-0485(1997)027<1038:KOTPEU>2.0.CO;2
- Bleck, R., Halliwell, G., Wallcraft, A., Carroll, S., Kelly, K., and Rushing, K. (2002). *HYCOM User's Manual v2.0.01*. Available at: https://www.hycom.org/attachments/063_hycom_users_manual.pdf.
- Brickman, D., and Taylor, L. (2007). Optimized biophysical model. *Fisheries* 16, 448e458. doi: 10.1111/j.1365-2419.2007.00449.x
- Cheng, Y., Putrasahan, D., Beal, L., and Kirtman, B. (2016). Quantifying Agulhas leakage in a high-resolution climate model. *J. Climate* 29, 6881–6892. doi: 10.1175/JCLI-D-15-0568.1
- Diaz, H., Folland, C., Manabe, P., Reynolds, D., and Woodruff, S. (2002). Workshop on advances in the use of historical marine climate data. *Bull. World Meteorological Organ.* 51 (4), 377–380.
- Durgadoo, J. V., uhs, S. R., Biastoch, A., and Böning, C. W. B. (2017). Indian Ocean sources of Agulhas leakage. *J. Geophys. Res. Oceans* 122, 3481–3499. doi: 10.1002/2016JC012676
- Egbert, G. D., and Erofeeva, S. Y. (2002). Efficient inverse modeling of barotropic ocean tides. *J. Atmos. Oceanic Technol.* 19, 183–204. doi: 10.1175/1520-0426(2002)019<0183:EIMOBO>2.0.CO;2
- Fang, G. H., Susanto, R. D., Wirasantosa, S., Qiao, F., Supangat, A., Fan, B., et al. (2010). Volume, heat, and freshwater transports from the South China Sea to Indonesian seas in the boreal winter of 2007–2008. *J. Geophys. Res. Oceans* 115, C12020. doi: 10.1029/2010JC006225
- Fang, G., Wang, Y., Wei, Z., Fang, Y., Qiao, F., and Hu, X. (2009). Inter-ocean circulation and heat and freshwater budgets of the South China Sea based on a numerical model. *Dyn. Atmos. Oceans* 47, 55–72. doi: 10.1016/j.dynatmoce.2008.09.003
- Ffield, A., and Gordon, A. L. (1992). Vertical mixing in the Indonesian thermocline. *J. Phys. Oceanogr.* 22, 184–195. doi: 10.1175/1520-0485(1992)022<0184:VMITIT>2.0.CO;2
- Ffield, A., and Gordon, A. L. (1996). Tidal mixing signatures in the Indonesian Seas. *J. Phys. Oceanogr.* 26, 1924–1937. doi: 10.1175/1520-0485(1996)026<1924:TMSITI>2.0.CO;2
- Fioux, M., Andrié, C., Delecluse, P., Ilahude, A. G., Kartavtseff, A., Mantis, F., et al. (1994). Measurements within the Pacific-Indian oceans throughflow region. *Deep-Sea Res.* 41, 1091–1130. doi: 10.1016/0967-0637(94)90020-5
- Gao, G., Yang, D., Xu, L., Zhang, K., Feng, X., and Yin, B. (2022). A biological-parameter-optimized modeling study of physical drivers controlling seasonal

Conflict of interest

The authors declare that the research was conducted in the absence of any commercial or financial relationships that could be construed as a potential conflict of interest.

Publisher's note

All claims expressed in this article are solely those of the authors and do not necessarily represent those of their affiliated organizations, or those of the publisher, the editors and the reviewers. Any product that may be evaluated in this article, or claim that may be made by its manufacturer, is not guaranteed or endorsed by the publisher.

Supplementary material

The Supplementary Material for this article can be found online at: <https://www.frontiersin.org/articles/10.3389/fmars.2023.1326048/full#supplementary-material>

chlorophyll blooms off the southern coast of Java Island. *J. Geophys. Res. Oceans* 127, e2022JC018835. doi: 10.1029/2022JC018835

Godfrey, J. S. (1996). The effect of the Indonesian throughflow on ocean circulation and heat exchange with the atmosphere: a review. *J. Geophys. Res.* 101, 12217–12237. doi: 10.1029/95JC03860

Gordon, A. L. (2005). Oceanography of the Indonesian seas and their throughflow. *Oceanography* 18, 14–27. doi: 10.5670/oceanog.2005.01

Gordon, A. L., and Fine, R. A. (1996). Pathways of water between the Pacific and Indian oceans in the Indonesian seas. *Nature* 379, 146–149. doi: 10.1038/379146a0

Gordon, A. L., Giulivi, C. F., and Ilahude, A. G. (2003). Deep topographic barriers within the Indonesian Seas. *Deep-Sea Res. II* 50, 2205–2228. doi: 10.1016/S0967-0645(03)00053-5

Gordon, A. L., Huber, B. A., Metzger, E. J., Susanto, D., Hurburt, H., and Adi, R. (2012). South China Sea throughflow impact on the Indonesian throughflow. *Geophys. Res. Lett.* 39, L11602. doi: 10.1029/2012GL052021

Gordon, A. L., Sprintall, J., Van Aken, H. M., Susanto, D., Wijffels, S., Molcard, R., et al. (2010). The Indonesian throughflow during 2004–2006 as observed by the INSTANT program. *Dynamics Atmospheres Oceans* 50, 115–128. doi: 10.1016/j.dynatmoce.2009.12.002

Gordon, A. L., Susanto, R. D., and Ffield, A. (1999). Throughflow within Makassar Strait. *Geophys. Res. Lett.* 26, 3325–3328. doi: 10.1029/1999GL002340

Gordon, A. L., Susanto, R. D., Ffield, A., Huber, B. A., Pranowo, W., and Wirasantosa, S. (2008). Makassar Strait throughflow 2004 to 2006. *Geophys. Res. Lett.* 35, L24605. doi: 10.1029/2008GL036372

Guo, Y., Li, Y., and Wang, F. (2023). Destinations and pathways of the Indonesian throughflow water in the Indian Ocean. *J. Climate* 36, 3717–3735. doi: 10.1175/JCLI-D-22-0631.1

Haidvogel, D. B., Arango, H., Hedstrom, K., Beckmann, A., Malanotte-Rizzoli, P., and Shchepetkin, A. (2000). Model evaluation experiments in the North Atlantic Basin: Simulations in nonlinear terrain-following coordinates. *Dyn. Atmos. Oceans* 32, 239–281. doi: 10.1016/S0377-0265(00)00049-X

Hautala, S., Reid, J., and Bray, N. (1996). The distribution and mixing of Pacific water masses in the Indonesian seas. *J. Geophys. Res.* 101, 375–312. doi: 10.1029/96JC00037

Hautala, S. L., Sprintall, J., Potemra, J., Chong, J. C., Pandoe, W., Bray, N., et al. (2001). Velocity structure and transport of the Indonesian throughflow in the major straits restricting flow into the Indian Ocean. *J. Geophys. Res.* 106, 19527–19546. doi: 10.1029/2000JC000577

Iskandar, M. R., Jia, Y., Sasaki, H., Furue, R., Kida, S., Suga, T., et al. (2023). Effects of high-frequency flow variability on the pathways of the Indonesian Throughflow. *J. Geophys. Res. Oceans* 128, e2022JC019610. doi: 10.1029/2022JC019610

- Kartadikaria, A. R., Miyazawa, Y., Nadaoka, K., and Watanabe, A. (2012). Existence of eddies at crossroad of the Indonesian seas. *Ocean Dynamics* 62, 31–44. doi: 10.1007/s10236-011-0489-1
- Koch-Larrouy, A., Madec, G., Iudicone, D., Atmadipoera, A., and Molcard, R. (2008). Physical processes contributing to the water mass transformation of the Indonesian Throughflow. *Ocean Dynamics* 58, 275–288. doi: 10.1007/s10236-008-0154-5
- Lebedev, K. V., and Yaremchuk, M. (2000). A diagnostic study of the Indonesian Throughflow. *J. Geophys. Res.* 105, 11243–11258. doi: 10.1029/2000JC900015
- Lee, T., Fournier, S., Gordon, A. L., and Sprintall, J. (2019). Maritime Continent water cycle regulates low-latitude chokepoint of global ocean circulation. *Nat. Commun.* 10, 2103. doi: 10.1038/s41467-019-10109-z
- Lee, T., Fukumori, I., Menemenlis, D., Xing, Z., and Fu, L.-L. (2002). Effects of the Indonesian throughflow on the Pacific and Indian oceans. *J. Phys. Oceanogr.* 32, 1404–1429. doi: 10.1175/1520-0485(2002)032<1404:EOTITTO>2.0.CO;2
- Liang, L., Xue, H., and Shu, Y. (2019). The Indonesian throughflow and the circulation in the Banda sea: a modeling study. *J. Geophys. Res.: Oceans* 124, 3089–3106. doi: 10.1029/2018JC014926
- Locarnini, R. A., Mishonov, A. V., Antonov, J. L., Boyer, T. P., Garcia, H. E., Baranova, O. K., et al. (2013). “World ocean atlas 2013,” in *Volume 1: Temperature*, vol. 73. Ed. S. Levitus (NOAA Atlas NESDIS 73: NOAA Atlas NESDIS), 40. A. Mishonov, Technical Ed.
- Luick, J. L., and Cresswell, G. R. (2001). Current measurements in the Maluku sea. *J. Geophys. Res. Oceans* 106, 13953–13958. doi: 10.1029/2000JC000694
- Masumoto, Y., and Yamagata, T. (1996). Seasonal variations of the Indonesia Throughflow in a general ocean circulation model. *J. Geophys. Res.* 101, 12287–12293. doi: 10.1029/95JC03870
- Miyama, T., Awaji, T., Akitomo, K., and Imasato, N. (1995). Study of seasonal transport variations in the Indonesian seas. *J. Geophys. Res. Atmospheres* 100, 20517–20542. doi: 10.1029/95JC01667
- Molcard, R., Fieux, M., and Syamsudin, F. (2001). The throughflow within ombai strait. *Deep-Sea Res. Part I* 48, 1237–1253. doi: 10.1016/S0967-0637(00)00084-4
- Paris, C. B., Helgers, J., Sebille, E. V., and Srinivasan, A. (2013). Connectivity modeling system: a probabilistic modeling tool for the multi-scale tracking of biotic and abiotic variability in the ocean. *Environ. Model. Softw.* 42, 47–54. doi: 10.1016/j.envsoft.2012.12.006
- Potemra, J. T., Hautala, S. L., and Sprintall, J. (2003). Vertical structure of Indonesian throughflow in a large-scale model. *Deep-sea Res. Part II* 50, 2143–2161. doi: 10.1016/S0967-0645(03)00050-X
- Pujiana, K., Gordon, A. L., Sprintall, J., and Susanto, R. D. (2009). Intraseasonal variability in Makassar Strait thermocline. *J. Mar. Res.* 67, 757–777. doi: 10.1357/002224009792006115
- Purba, N. P., Faizal, I., Damanik, F. S., Rachim, F. R., and Mulyani, P. G. (2020). Overview of oceanic eddies in Indonesia seas based on the sea surface temperature and sea surface height. *World Sci. News* 147, 166–178.
- Purba, N. P., and Khan, A. M. A. (2019). Upwelling session in Indonesia waters. *World News Nat. Sci.* 25, 72–83.
- Qin, X., van Sebille, E., and Sen Gupta, A. (2014). Quantification of errors induced by temporal resolution on Lagrangian particles in an eddy-resolving model. *Ocean Modell.* 76, 20–30. doi: 10.1016/j.ocemod.2014.02.002
- Qu, T., Du, Y., Meyers, G., Ishida, A., and Wang, D. (2005). Connecting the tropical Pacific with Indian Ocean through South China Sea. *Geophys. Res. Lett.* 32, L24609. doi: 10.1029/2005GL024698
- Qu, T., Du, Y., and Sasaki, H. (2006). South China Sea Throughflow: A heat and freshwater conveyor. *Geophys. Res. Lett.* 33, L23617. doi: 10.1029/2006GL028350
- Qu, T., Song, Y. T., and Yamagata, T. (2009). An introduction to the South China Sea throughflow: Its dynamic, variability, and application for climate. *Dyn. Atmos. Oceans* 47, 3–14. doi: 10.1016/j.dynatmoce.2008.05.001
- Richardson, P. L. (1983). Eddy kinetic energy in the North Atlantic from surface drifters. *J. Geophys. Res.* 88, 4355–4436. doi: 10.1029/JC088iC07p04355
- Robertson, R., and Ffield, A. (2008). Baroclinic tides in the Indonesian seas: Tidal fields and comparisons to observations. *J. Geophys. Res.* 113, C07031. doi: 10.1029/2007JC004677
- Rühs, S., Durgadoo, J. V., Behrens, E., and Biastoch, A. (2013). Advective timescales and pathways of Agulhas leakage. *Geophys. Res. Lett.* 40, 3997–4000. doi: 10.1002/grl.50782
- Shchepetkin, A. F., and McWilliams, J. C. (2005). The regional oceanic modeling system (ROMS): A split-explicit, free-surface, topography-following-coordinate oceanic model. *Ocean Modell.* 9, 347–404. doi: 10.1016/j.ocemod.2004.08.002
- Sprintall, J., Gordon, A., Koch-Larrouy, A., Lee, T., Potemra, J. T., Pujiana, K., et al. (2014). The Indonesian seas and their role in the coupled ocean–climate system. *Nat. Geosci.* 7, 487–492. doi: 10.1038/ngeo2188
- Sprintall, J., Gordon, A. L., Wijffels, S. E., Feng, M., Hu, S., Koch-Larrouy, A., et al. (2019). Detecting change in the Indonesian seas. *Front. Mar. Sci.* 6. doi: 10.3389/fmars.2019.00257
- Sprintall, J., Wijffels, S. E., Molcard, R., and Jaya, I. (2009). Direct estimates of the Indonesian throughflow entering the Indian Ocean: 2004–2006. *J. Geophys. Res.* 114, C07001. doi: 10.1029/2008JC005257
- Susanto, R. D., Ffield, A., Gordon, A. L., and Adi, T. R. (2012). Variability of Indonesian throughflow within Makassar Strait 2004–2009. *J. Geophys. Res. Oceans* 117, C09013. doi: 10.1029/2012JC008096
- Susanto, R. D., and Gordon, A. L. (2005). Velocity and transport of the Makassar Strait throughflow. *J. Geophys. Res. Oceans* 110, C01005. doi: 10.1029/2004JC002425
- Susanto, R. D., Wei, Z., Adi, R. T., Fan, B., Li, S., and Fang, G. (2013). Observations of the karimata strait throughflow from december 2007 to november 2008. *Acta Oceanologica Sin.* 32, 1–6. doi: 10.1007/s13131-013-0307-3
- Talley, L. D., and Sprintall, J. (2005). Deep expression of the Indonesian Throughflow: Indonesian intermediate water in the South equatorial current. *J. Geophys. Res. Oceans* 110, C10009. doi: 10.1029/2004JC002826
- Taufiqurrahman, E., Wahyudi, A., and Masumoto, Y. (2020). The Indonesian throughflow and its impact on biogeochemistry in the Indonesian seas. *Asean J. Sci. Technol. Dev.* 37, 29–35–29–35. doi: 10.29037/ajstd.596
- Tozuka, T., Qu, T. D., Masumoto, Y., and Yamagata, T. (2009). Impacts of the South China Sea Throughflow on seasonal and interannual variations of the Indonesian Throughflow. *Dyn. Atmos. Oceans* 47, 73–85. doi: 10.1016/j.dynatmoce.2008.09.001
- Tozuka, T., Qu, T., and Yamagata, T. (2007). Dramatic impact of the south China sea on the Indonesian throughflow. *Geophys. Res. Lett.* 34, L12612. doi: 10.1029/2007GL030420
- Van Aken, H. M., Brodjonegoro, I. S., and Jaya, I. (2009). The deep-water motion through the Lifamatola Passage and its contribution to the Indonesian throughflow. *Deep Sea Res. Part I: Oceanographic Res. Papers* 56, 1203–1216. doi: 10.1016/j.dsr.2009.02.001
- Van Aken, H. M., Punjawan, J., and Saimima, S. (1988). Physical aspects of the flushing of the East Indonesian basins. *Neth. J. Sea Res.* 22, 315–339. doi: 10.1016/0077-7579(88)90003-8
- van Sebille, E., England, M. H., Zika, J. D., and Sloyan, B. M. (2012). Tasman leakage in a fine-resolution ocean model. *Geophys. Res. Lett.* 39, L06660. doi: 10.1029/2012GL051004
- van Sebille, S. J., Schwarzkopf, F. U., Sen Gupta, A., Santoso, A., England, M. H., Biastoch, A., et al. (2014). Pacifico-Indian Ocean connectivity: Tasman leakage, Indonesian Throughflow, and the role of ENSO. *J. Geophys. Res. Oceans* 119, 1365–1382. doi: 10.1002/2013JC009525
- Vranes, K., Gordon, A. L., and Ffield, A. (2002). The heat transport of the Indonesian throughflow and implications for the Indian Ocean heat budget. *Deep Res. Part II* 49, 1391–1410. doi: 10.1016/S0967-0645(01)00150-3
- Wajsowicz, R. C. (1996). Flow of a western boundary current through multiple straits: An electrical circuit analogy for the Indonesian Throughflow and archipelago. *J. Geophys. Res. Oceans* 101, 12295–12300. doi: 10.1029/95JC02615
- Wajsowicz, R. C., and Schneider, E. K. (2001). The Indonesian throughflow’s effect on global climate determined from the COLA Coupled Climate System. *J. Climate* 14, 3, 029–3,042. doi: 10.1175/1520-0442(2001)014<3029:TITSEO>2.0.CO;2
- Wang, D. X., Liu, Q. Y., Huang, R. X., Du, Y., and Qu, T. (2006). Interannual variability of the South China Sea throughflow inferred from wind data and an ocean data assimilation product. *Geophys. Res. Lett.* 33, L14605. doi: 10.1029/2006GL026316
- Wang, L., Xie, L. L., Zhou, L., Li, Q., Shi, Y., and Li, M. (2018). Climatological analysis of water mass sources of Indonesia Throughflow in the Molukka Sea and Halmahera Sea. *Haiyang Xuebao (in Chinese)* 40, 1–15. doi: 10.3969/j.issn.0253-4193.2018.03.001
- Wang, L., Zhou, L., Xie, L., Zheng, Q., Li, Q., and Li, M. (2019). Seasonal and interannual variability of water mass sources of Indonesian throughflow in the Maluku Sea and the Halmahera Sea. *Acta Oceanol. Sin.* 38, 58–71. doi: 10.1007/s13131-019-1413-7
- Wattimena, M. C., Atmadipoera, A. S., Purba, M., Nuijaya, I. W., and Syamsudin, F. (2018). Indonesian Throughflow (ITF) variability in Halmahera Sea and its coherency with New Guinea Coastal Current IOP Conf. Series: Earth Environ. Sci. 176, 2018012011. doi: 10.1088/1755-1315/176/1/012011
- Weijer, W., Sloyan, B. M., Maltrud, M. E., Jeffery, N., Hecht, M. W., Hartin, C. A., et al. (2012). The Southern Ocean and its climate in CCSM4. *J. Climate* 25, 2652–2675. doi: 10.1175/JCLI-D-11-00302.1
- Wyrtki, K. (1961). Physical oceanography of the Southeast Asian waters La Jolla. *Univ. California Scripps Institution Oceanography*.
- Yuan, D., Yin, X., Li, X., Corvianawatie, C., Wang, Z., Li, Y., et al. (2022). A Maluku Sea intermediate western boundary current connecting Pacific Ocean circulation to the Indonesian Throughflow. *Nat. Commun.* 13, 2093. doi: 10.1038/s41467-022-29617-6